Dalton Transactions

ROYAL SOCIETY OF CHEMISTRY

COMMUNICATION

View Article Online
View Journal | View Issue

Cite this: *Dalton Trans.*, 2020, **49**, 4694

Received 3rd March 2020,
Accepted 13th March 2020

DOI: 10.1039/d0dt00801j

rsc.li/dalton

Six-coordinate mononuclear dysprosium(III) single-molecule magnets with the triphenylphosphine oxide ligand†

Kuduva R. Vignesh, Dimitris I. Alexandropoulos, Haomiao Xie and Kim R. Dunbar *

Structural, magnetic and theoretical studies of three octahedral mononuclear Dy^{III} complexes with triphenylphosphine oxide and halide ligands are reported. The Cl^- and Br^- analogues exhibit SMM behavior with energy barriers of 49.1 K and 70.9 K, respectively under a small dc field. *Ab initio* calculations were performed, the results of which predict higher energy barriers for iodide containing SMMs.

Increasing the magnetic anisotropy in mononuclear lanthanide complexes is an important challenge in molecular magnetism. An effective method to raise the magnetization reversal barrier (U_{eff}) of mononuclear lanthanide single-molecule magnets (SMMs) with oblate electron density of the 4f orbitals is to enforce a strongly axial coordination environment.[1] The most prominent 4f ions in the oblate category are Tb(III) and Dy(III) which have been used to design low-coordinate axial complexes that exhibit extraordinarily high blocking temperatures,[2] a fact that makes them targets of interest for data storage and processing.[3] The axial nature of the ligand field controls both the magnitude of U_{eff} and the probability of quantum tunnelling of the magnetization (QTM) between the low-lying magnetic states.[4] The ability to enforce axial symmetry is imperative for controlling the slow magnetic relaxation and, therefore, achieving higher blocking temperatures.[5] Indeed, design of rare earth complexes with these principles in mind has led to remarkable advances in blocking temperatures (T_B), especially for mononuclear Dy(III) SMMs with $C_{\infty v}$, $D_{\infty h}$, $S_8(I_4)$, D_{4d}, and D_{5h} symmetries.[1,2,6] Excellent examples of such compounds are pentagonal bipyramidal (PBP) Dy(III) complexes[6a–c] and Dy(III) metallocenium complexes that exhibit hysteresis in the range of 60 K to 80 K.[2]

Of particular relevance to the present study is the fact that only one six-coordinate mononuclear Ln(III) SMM has been reported that exhibits SMM behaviour in the absence of an applied field.[7] This situation is a consequence of fast quantum tunnelling in octahedral SMMs with D_{4d} symmetry. Calculations, however, predict that lowering the symmetry from an ideal octahedron will quench the QTM and produce large U_{eff} barriers.[8] In this vein, complexes with weak equatorial and stronger axial ligands are good targets.

Herein we report the synthesis, magnetic properties and theoretical analysis of three octahedral (O_h) compounds. Reactions of anhydrous DyX_3 (X = Cl, Br and I) and Ph_3PO in a 2 : 1 molar ratio in THF produce pale yellow crystals of $[Dy^{III}X_3(OPPh_3)_2(THF)]\cdot THF$ (X = Cl (**1**) and Br(**2**)) (Ph_3PO = triphenylphosphine oxide, THF = tetrahydrofuran) and $[Dy^{III}I_2(OPPh_3)_4]I\cdot 4THF\cdot 0.3H_2O$ (**3**). The chemical and structural characteristics of the compounds were confirmed by single-crystal X-ray crystallography (Table S1†), elemental analyses (C, H, N), and IR spectral data (ESI). The presence of an equatorial THF ligand in **1** and **2** diminishes the D_{4d} symmetry, and the bulky phosphine oxide ligands contribute to a lower coordination number and exert a stronger ligand field in the axial positions.[9]

Compounds **1** and **2** are isostructural and crystallize in the triclinic space group $P\bar{1}$ with asymmetric units that contain one $[DyCl_3(OPPh_3)_2]$ (Fig. 1) or $[DyBr_3(OPPh_3)_2]$ (Fig. S1†) moiety, and an interstitial THF solvent molecule. The Dy^{III} ions in **1** and **2** are six-coordinate with three chlorides or bromides, one THF, and two $OPPh_3$ ligands. Compound **3** crystallizes in the monoclinic space group $P21/c$. The structure contains well-separated $[DyI_2(OPPh_3)_4]^+$ cations and iodide anions with disordered interstitial THF and H_2O solvent molecules. The Dy^{III} ion is six-coordinate with two iodide ions and four $OPPh_3$ ligands. The average Dy–X (X = Cl, Br, I) distances are 2.6150(6) for **1**, 2.7743(3) for **2** and, 3.0287(8) for **3** which are significantly longer than the corresponding Dy–O bonds of 2.3227(2), 2.266(2) and 2.225(7), respectively. The crystal packing diagram of **1–3** reveals well-isolated moieties with the

Department of Chemistry, Texas A&M University, College Station, Texas 77842-3012, USA. E-mail: dunbar@chem.tamu.edu

†Electronic supplementary information (ESI) available: Synthetic, crystallographic, magnetic and computational details. CCDC 1916601–1916603. For ESI and crystallographic data in CIF or other electronic format see DOI: 10.1039/d0dt00801j

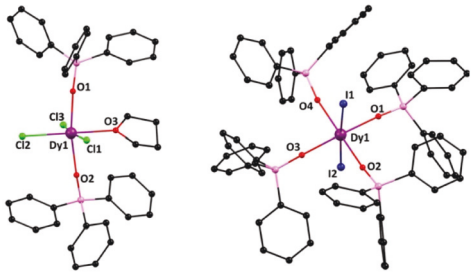

Fig. 1 Crystal structures of **1** (left) and cation **3** (right). H atoms were omitted for the sake of clarity. Colour scheme: Dy, purple; O, red; Cl, green; I, dark blue; C, black.

closest intermolecular Dy···Dy contacts being 8.575(2) Å, 8.617(5) Å and, 10.923(5) Å, for **1**, **2** and **3**, respectively.

In order to evaluate the symmetry of the inner coordination spheres of the dysprosium ions in **1–3**, SHAPE[10] calculations were performed (Table S2†). The results reveal that Dy1 in **1–3** adopts a distorted octahedral geometry (CShM: 0.85, 1.40, and 2.50, for **1**, **2** and **3**, respectively). In **1** and **2**, the two $OPPh_3$ ligands occupy the axial positions of the octahedron while the equatorial plane is filled by three halides and one oxygen atom. In **3**, the octahedral coordination environment of Dy1 consists of two axial iodide ligands adopting a *trans* arrangement and four oxygen atoms in the equatorial plane. Deviations from an ideal O_h symmetry in **1–3** are evidenced by the X–Dy–X (X = Cl, Br, I) and O–Dy–O angles which are X–Dy–X: 170.95(2)°, 171.24(2)°, 176.50(3)° and O–Dy–O: 170.36(2)°, 174.40(2)° and, 173.15(3)° (average values) for **1**, **2** and **3**, respectively, as well as the puckering of the equatorial plane.[11]

DC magnetic studies were conducted on **1–3** in a 0.1 T field over the temperature range 2–300 K (Fig. 2). The room temperature values of 14.02, 14.00 and 13.53 $cm^3\ mol^{-1}\ K$ for **1**, **2** and **3**, respectively are consistent with the expected value of 14.17 $cm^3\ mol^{-1}\ K$ for an isolated Dy^{III} ($4f^9$, $^6H_{15/2}$, $S = 5/2$, $L = 5$, $g = 4/3$) ion. The $\chi_M T$ value decreases gradually for **3** and reaches 10.55 $cm^3\ mol^{-1}\ K$ at 2 K in a field of 0.1 T, and, for **1** and **2**, $\chi_M T$ decreases from 300 K to values of 13.42 and 13.56 $cm^3\ mol^{-1}\ K$ at 100 K and 12.20 and 12.30 $cm^3\ mol^{-1}\ K$ at 2 K for **1** and **2**, respectively. The sharper decrease below

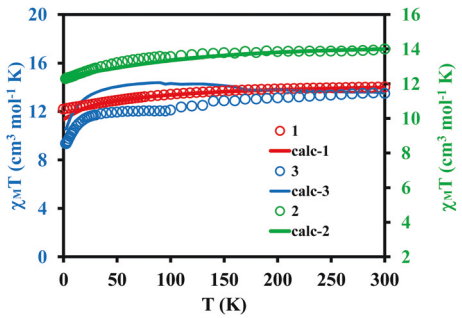

Fig. 2 $\chi_M T$ *vs.* T for **1–3** with an applied magnetic field of 0.1 T. The solid colour lines are *ab initio* calculated magnetic susceptibility values.

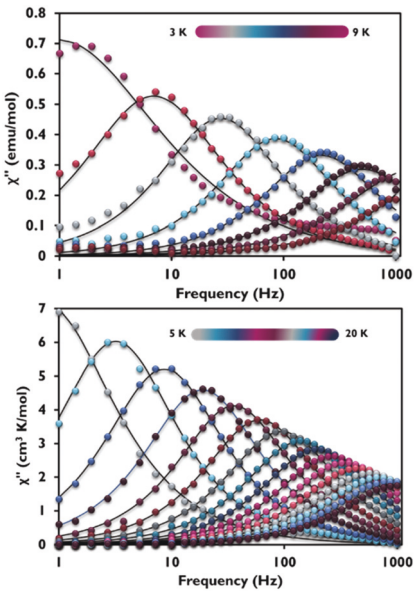

Fig. 3 χ''_M *vs.* frequency for **1** (top) and **2** (bottom) at H_{dc} = 400 Oe.

100 K for **1** and **2** is attributed to the presence of magnetic anisotropy and/or depopulation of the m_J levels arising from the crystal field levels of the Dy^{III} ions. This conclusion is further supported by the *M vs. H* plots, for which the molar magnetization does not saturate at 7 T, but rather exhibits a near linear dependence above 2 T (Fig. S2†).

Ac magnetic studies also were performed on **1–3** and it was found that the χ''_M *vs.* T plots do not exhibit out-of-phase susceptibility signals in the absence of an applied static dc field, with the exception of a very slightly frequency dependence for **2** (Fig. S3†). Upon application of a static field of H_{dc} = 400 Oe, however, SMM behaviour is observed for **1** and **2** (Fig. S4†). Frequency dependent maxima are observed from 3 to 9 K For **1** and from 5 to 20 K for **2** (Fig. 3).

The relaxation data for **1** and **2** were fit with the CC-FIT program[12] (Fig. 4) using the equation, $[1/\tau = 1/\tau_{QTM} + CT^n + \tau_o^{-1} \exp(U_{eff}/k_B T)]$ where $1/\tau_{QTM}$ relates to the relaxation process *via* QTM pathway, the CT^n term relates to the relaxation *via* Raman process, and the last term accounts for the Orbach relaxation pathway.[13] The values obtained from the best fit are n = 6.4, C = 0.003 $s^{-1}\ K^{-6.4}$, U_{eff} = 49.1 K and τ_o = 2.0×10^{-6} s for **1**, and n = 4.3, C = 0.0002 $s^{-1}\ K^{-4.3}$, U_{eff} = 70.9 K and $\tau_o = 1.6 \times 10^{-6}$ s for **2** (Fig. 4). A QTM relaxation times, τ_{QTM}, of 0.05 s and 0.02 s were estimated for **1** and **2**, respectively.

To probe the electronic structure and magnetic anisotropy of the Dy^{III} ions in **1–3** and account for the observed static and dynamic magnetic behaviour, detailed *ab initio* CASSCF/RASSI/SINGLE_ANISO calculations were performed. The ground state Kramers doublets (KDs) of complexes **1** and **2** have small transverse components (g_x, g_y) and the g_z values nearly of ~20 expected for the pure Ising $|m_J = 15/2|$ multiplet (Tables 1 and S5†). These results indicate that these molecules should exhibit slow relaxation of the magnetization either at zero field

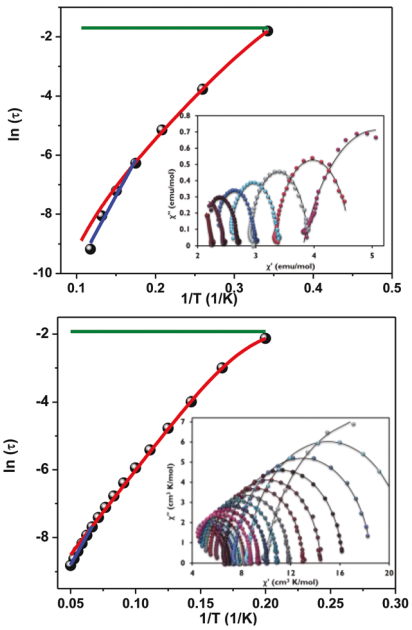

Fig. 4 Magnetization relaxation time (τ), plotted as ln τ *vs.* T^{-1} for (top) **1** and (bottom) **2**. The solid blue line corresponds to the fitting of the Orbach relaxation process, and the solid red line represents the fitting to multiple relaxation processes. The horizontal green line represents the QTM relaxation time. (Insets) Cole–Cole plots to the respective complexes. The black solid lines are fitted data extracted from CC-FIT program.[12]

Table 1 *Ab initio* computed eight low-lying Kramers doublet energies (cm^{-1}) and g-tensors of ground Kramers doublet in compounds **1–4**

KDs	1	2	3	4
1	0.0	0.0	0.0	0.0
2	147.3	234.9	46.1	272.5
3	196.3	332.3	217.1	427.3
4	225.8	358.5	312.1	475.7
5	360.9	465.3	460.7	586.1
6	394.6	511.9	573.3	612.7
7	435.3	551.7	591.3	665.3
8	474.3	591.7	641.9	694.9
g_x	0.0545	0.0062	0.2921	0.0016
g_y	0.1326	0.0111	1.0878	0.0031
g_z	19.7570	19.9166	19.0160	19.9201

or under the application of a small dc field, in accord with experimental observations for **1** and **2** which exhibit SMM behaviour under an applied field of 400 Oe. In contrast, the large transverse component observed for **3** in the ground KD predicts an absence of SMM behaviour (Tables 1 and S6†), as confirmed by experiment. The *ab initio* computed magnetic susceptibility (Fig. 2) and isothermal magnetization (Fig. S2†) data are in good agreement with the experimental magnetic data, which supports the computed parameters.

The ground state g_{zz} axis in **1** and **2** is found to be aligned along the O-atoms of two Ph_3PO ligands (Fig. S4†) in the axial positions. This is mainly due to the fact that the oblate Dy^{III} electron density is preferentially located perpendicular to the shortest Dy–O (2.23 to 2.32 Å) bond distances of the Ph_3PO ligand compared to the Dy–X (2.62 to 3.03 Å) distances of the halides. In the case of **3**, the parallel orientation of the ground state g_{zz} tensor with respect to the Dy^{III} electron density is observed which is further supported with the Loprop charge analysis[14] which indicates large negative charges on the Ph_3PO O-atoms (−1.10 to −1.12) and small negative charges for the halide ions (−0.87 for Cl, −0.85 for Br and −0.79 for I). For the Dy^{III} ion, very strong axial ligands are necessary along with weak equatorial ligands for large ground-first excited state gap.[6a,b] Such a situation is present in **1** and **2**, but is absent in **3**. Thus, for **1** and **2**, calculations predict an energy gap of 147.3 and 234.9 cm^{-1} between the ground and first excited KDs, respectively (Table 1). Compound **3**, which contains Ph_3PO ligands in equatorial position and weak iodide ligands in the axial position is predicted to have a very small energy gap (46.1 cm^{-1}).

To determine the energy barrier for each complex, relaxation mechanisms were constructed for the magnetization blockade (Fig. 5 and S6†). In **1** and **2**, the ground state quantum tunnelling of the magnetization (QTM) process is found to be small (0.03, and 0.003μ_B for **1** and **2** respectively) which allows the magnetization to relax *via* excited states. The wave function analysis predicts that the ground KDs are primarily composed of the 15/2 state with small contributions from other states for **1** and **2**. However, the enhanced transverse components at first excited KD leads to large thermally

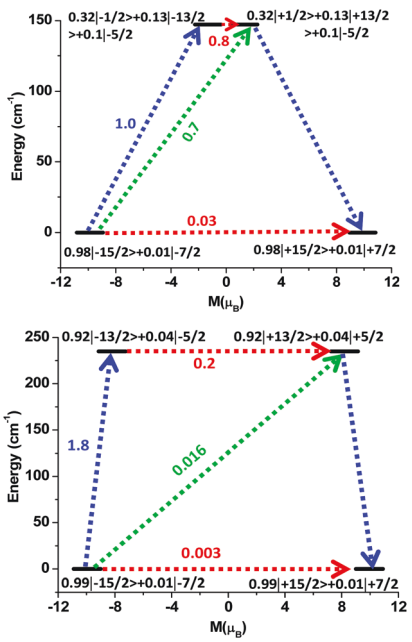

Fig. 5 *Ab initio* computed magnetization blocking barrier for (top) **1** and (bottom) **2**. The thick black line indicates the KDs as a function of the computed magnetic moment. The green/blue arrows show the possible pathway through Orbach/Raman relaxation. The red lines represent the presence of QTM/TA-QTM between the connecting pairs. The numbers provided at each arrow are the mean absolute values for the corresponding matrix element of the transition magnetic moment.

assisted QTM (TA-QTM) processes (0.8 and 0.2μ_B for **1** and **2**, respectively) and this situation allows for magnetic relaxation *via* the first excited states which lie at 147.3 cm^{-1} (212 K) for **1** and 234.9 cm^{-1} (338 K) for **2**. These computational results rationalize the experimentally observed frequency-dependent χ''_M maxima for **1** and **2** in the presence of a small DC field (400 Oe). The experimental energy barriers are relatively lower than calculated values which is attributed to the exclusion of intermolecular and hyperfine interactions in the calculation and the fact that relaxation mechanisms such as spin-phonon relaxation are possible which have not be taken into consideration.[9c,13b] The ground state QTM is operative for **3** and this is attributed to the ground KD is mostly mixed with all the m_J states and allow the magnetization to relax *via* ground state itself (Fig. S6†). Not surprisingly, no out-of-phase susceptibility signals for **3**, even upon application of a dc field were observed. To provide further insight into the mechanism of magnetic relaxation, the crystal field parameters were calculated (Table S7†). In the case of **1** and **2**, the axial B_k^q terms (q = 0 and k = 2, 4) are moderately larger than the two non-axial terms, which leads to relatively weaker QTM in the ground state.[9c,13b] For **3**, the non-axial terms are larger than the axial terms which explains the computed transverse anisotropy and the corresponding QTM probabilities in the ground state.

At this point it is interesting to ask whether the Iodide ions in a similar octahedral geometry for the Dy^{III} ion as **1** and **2** would exhibit large anisotropy barrier heights.[6a,9c] To address this question, a model octahedral complex with the Ph_3PO and I ligands, namely $[Dy^{III}(OPPh_3)_2(THF)I_3]^-$ (**4**) was subjected to computations. The calculations predict negligible transverse components and extremely small QTM values in the ground KD for **4** than what was found for **1** and **2** as expected due to the weaker equatorial donation by the iodide ligand. The crystal field parameters support that the compound would exhibit small QTM values (Table S7†). Calculations suggest the magnetic relaxation would occur *via* the third KD (Table 1 and Fig. 6) which leads to an increased energy barrier of 427.3 cm^{-1} (614.8 K). Since the ground KD is purely a 15/2 state and the second KD is mostly the 13/2 state, the relaxation of magnetization occurs *via* the third KD at 427.3 cm^{-1} would likely be achieved in a zero dc field.[6a–c] These promising computational results provide good rationale for targeting six-coordinate Ln complexes and other low-coordinate Ln complexes with iodide atoms in the equatorial positions.

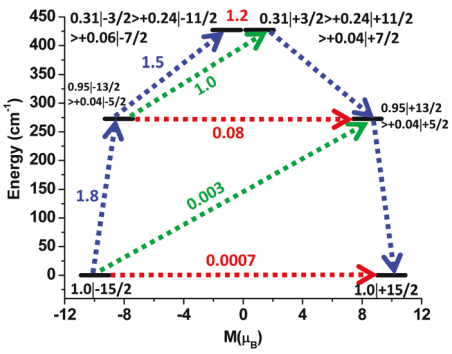

Fig. 6 *Ab initio* computed magnetization blocking barrier for **4**.

In this study, three new six-coordinate mononuclear Dy complexes bearing halide and TPPO ligands were evaluated by X-ray crystallography, magnetometry, and *ab initio* CASSCF calculations. The two compounds with axial TPPO ligands, a THF ligand and either a chloride (**1**) or a bromide (**2**) in the equatorial positions leads to slow magnetic relaxation at 49.1 K and 70.9 K, respectively due to the diminished D_{4d} symmetry. The improved energy barrier for **2** as compared **1** is due to the weaker ligand field of bromide *versus* chloride. Complex **3** exhibits a different coordination environment than **1** and **2** and does not exhibit SMM behaviour as confirmed by *ab initio* calculations. Work is in progress to synthesize six-coordinate Ln complexes with other weak equatorial ligands in tandem with strong axial donors.

Conflicts of interest

There are no conflicts to declare.

Acknowledgements

We gratefully acknowledge the National Science Foundation (CHE-1808779) and the Welch Foundation (A-1449) for financial support. We also thank the HPRC at Texas A&M University for the computing resources.

Notes and references

1 N. Ishikawa, M. Sugita, T. Ishikawa, S. Koshihara and Y. Kaizu, *J. Am. Chem. Soc.*, 2003, **125**, 8694–8695.
2 (*a*) C. A. P. Goodwin, F. Ortu, D. Reta, N. F. Chilton and D. P. Mills, *Nature*, 2017, **548**, 439–442; (*b*) F.-S. Guo, B. M. Day, Y.-C. Chen, M.-L. Tong, A. Mansikkamäki and R. A. Layfield, *Science*, 2018, **362**, 1400–1403; (*c*) F.-S. Guo, B. M. Day, Y.-C. Chen, M.-L. Tong, A. Mansikkamäki and R. A. Layfield, *Angew. Chem., Int. Ed.*, 2017, **56**, 11445–11449; (*d*) K. R. McClain, C. A. Gould, K. Chakarawet, S. J. Teat, T. J. Groshens, J. R. Long and B. G. Harvey, *Chem. Sci.*, 2018, **9**, 8492–8503.
3 (*a*) E. Coronado and A. J. Epsetin, *J. Mater. Chem.*, 2009, **19**, 1670–1671; (*b*) L. Bogani and W. Wernsdorfer, *Nat. Mater.*, 2008, **7**, 179–186; (*c*) M. N. Leuenberger and D. Loss, *Nature*, 2001, **410**, 789–793.
4 L. Thomas, F. Lionti, R. Ballou, D. Gatteschi, R. Sessoli and B. Barbara, *Nature*, 1996, **383**, 145.
5 (*a*) D. N. Woodruff, R. E. P. Winpenny and R. A. Layfield, *Chem. Rev.*, 2013, **113**, 5110–5148; (*b*) J. D. Rinehart, M. Fang, W. J. Evans and J. R. Long, *J. Am. Chem. Soc.*, 2011, **133**, 14236–14239; (*c*) J. D. Rinehart and J. R. Long, *Chem. Sci.*, 2011, **2**, 2078–2085.
6 (*a*) S. K. Gupta, T. Rajeshkumar, G. Rajaraman and R. Murugavel, *Chem. Sci.*, 2016, **7**, 5181–5191;

(*b*) Y.-C. Chen, J.-L. Liu, L. Ungur, J. Liu, Q.-W. Li, L.-F. Wang, Z.-P. Ni, L. F. Chibotaru, X.-M. Chen and M.-L. Tong, *J. Am. Chem. Soc.*, 2016, **138**, 2829–2837; (*c*) J. Liu, Y.-C. Chen, J.-L. Liu, V. Vieru, L. Ungur, J.-H. Jia, L. F. Chibotaru, Y. Lan, W. Wernsdorfer, S. Gao, X.-M. Chen and M.-L. Tong, *J. Am. Chem. Soc.*, 2016, **138**, 5441–5450; (*d*) N. Ishikawa, M. Sugita and W. Wernsdorfer, *Angew. Chem., Int. Ed.*, 2005, **44**, 2931–2935; (*e*) K. R. Meihaus and J. R. Long, *J. Am. Chem. Soc.*, 2013, **135**, 17952–17957; (*f*) A. K. Bar, P. Kalita, M. K. Singh, G. Rajaraman and V. Chandrasekhar, *Coord. Chem. Rev.*, 2018, **367**, 163–216.

7 M. Gregson, N. F. Chilton, A.-M. Ariciu, F. Tuna, I. F. Crowe, W. Lewis, A. J. Blake, D. Collison, E. J. L. McInnes, R. E. P. Winpenny and S. T. Liddle, *Chem. Sci.*, 2016, **7**, 155–165.

8 N. F. Chilton, *Inorg. Chem.*, 2015, **54**, 2097–2099.

9 (*a*) R. D. Bannister, W. Levason, G. Reid and W. Zhang, *Polyhedron*, 2017, **133**, 264–269; (*b*) J. Burt, W. Levason and G. Reid, *Coord. Chem. Rev.*, 2014, **260**, 65–115; (*c*) S. K. Langley, K. R. Vignesh, K. Holton, S. Benjamin, G. B. Hix, W. Phonsri, B. Moubaraki, K. S. Murray and G. Rajaraman, *Inorganics*, 2018, **6**, 61.

10 S. Alvarez, P. Alemany, D. Casanova, J. Cirera, M. Llunell and D. Avnir, *Coord. Chem. Rev.*, 2005, **249**, 1693–1708.

11 J. Long, A. N. Selikhov, E. Mamontova, K. A. Lyssenko, Y. Guari, J. Larionova and A. A. Trifonov, *Dalton Trans.*, 2019, **48**, 35–39.

12 N. F. Chilton, *CC-fit*, The Univesity of Manchester, UK, 2014, http://www.nfchilton.com/cc-fit.html.

13 (*a*) K. R. Vignesh, D. I. Alexandropoulos, B. S. Dolinar and K. R. Dunbar, *Dalton Trans.*, 2019, **48**, 2872–2876; (*b*) K. R. Vignesh, S. K. Langley, K. S. Murray and G. Rajaraman, *Inorg. Chem.*, 2017, **56**, 2518–2532.

14 L. Gagliardi, R. Lindh and G. Karlström, *J. Chem. Phys.*, 2004, **121**, 4494–4500.